

HEAT Repeats Mediate Plasma Membrane Localization of Tor2p in Yeast*

Received for publication, August 10, 2000

Published, JBC Papers in Press, September 5, 2000, DOI 10.1074/jbc.M007296200

Jeannette Kunz‡, Ulrich Schneider, Isabelle Howald, Anja Schmidt, and Michael N. Hall§

From the Department of Biochemistry, Biozentrum, University of Basel, Klingelbergstrasse 70, CH-4056 Basel, Switzerland

The subcellular distribution of Tor1p and Tor2p, two phosphatidylinositol kinase homologs and targets of the immunosuppressive drug rapamycin in *Saccharomyces cerevisiae*, was analyzed. We found that Tor protein is peripherally associated with membranes. Subcellular fractionation and immunofluorescence studies showed that Tor1p and Tor2p associate with the plasma membrane and a second fraction that is distinct from Golgi, vacuoles, mitochondria, and nucleus and may represent vesicular structures. Pulse-chase experiments showed that association of Tor protein with plasma membrane and the second compartment is fast, does not appear to involve components of endocytic, secretory, or Golgi to vacuole transport pathways, and is not affected by the immunosuppressive drug rapamycin. Deletion analysis reveals that two domains within Tor2p independently mediate localization to both compartments. These domains are composed of HEAT repeats that are thought to act as protein-protein interaction surfaces. Our studies therefore place Tor proteins at the site of action of their known downstream effectors and suggest that they may be part of a multiprotein complex.

The *Saccharomyces cerevisiae* Tor1p¹ and Tor2p proteins are components of a novel signaling pathway that controls cell growth in response to nutrient availability (1, 2). Tor1p and Tor2p were originally identified by dominant mutations that confer resistance to the immunosuppressive drug rapamycin, and were later shown to be the physical targets of the FKBP12-rapamycin complex (3–9). Tor1p and Tor2p are highly homologous and members of the phosphatidylinositol kinase-related kinase family (10). Phosphatidylinositol kinase-related kinases despite their homology to phosphatidylinositol 3- and 4-kinases are thought to function as protein kinases (11).

Tor2p is an essential protein that regulates cell growth in two ways. First, it acts redundantly with Tor1p in a nutrient-

sensing signaling cascade that is required for translation initiation and G₁ progression. This function is inhibited by rapamycin (1, 2). Second, Tor2p is also required for cell cycle-dependent reorganization of the actin cytoskeleton (12, 13). This function is unique to Tor2p, also essential, and is not sensitive to rapamycin. Accordingly, yeast cells lacking Tor1p and Tor2p activity or cells treated with rapamycin exhibit a dramatic reduction in translation initiation, and show all characteristics of nutrient-starved cells, including arrest in the early G₁ phase of the cell cycle, accumulation of the storage carbohydrate glycogen, degradation of amino acid transporters, transcriptional and morphological changes, down-regulation of ribosome biogenesis, and autophagy (14–20). Loss of Tor2p function alone, on the other hand, leads to arrest throughout the cell cycle and depolarization of the actin cytoskeleton (12, 13, 21).

The Tor signaling pathway appears to be evolutionarily conserved. The mammalian homolog mTOR, also known as FRAP/RAFT1/RAPT1, is highly related and acts in a rapamycin-sensitive signaling pathway that modulates translation initiation in response to mitogens or amino acid availability (2, 22–25). mTOR regulates translation by activating 70-kDa S6 kinase and inducing phosphorylation of the translational repressor 4E-BP1/PHAS-I which, in turn, leads to dissociation of 4E-BP from eIF4E and initiation of translation (1, 2, 26). So far, no direct role of mTOR in the regulation of actin dynamics has been demonstrated.

The mechanisms by which Tor coordinately regulates diverse cellular responses to nutrient availability are not precisely understood. Tor kinase activity controls the association of the phosphatase-associated factor Tap42p with type 2A and type 2A-related phosphatases (27–29). Tap42-mediated inhibition of phosphatase activity in turn prevents nuclear accumulation of nutrient-regulated transcription factors, inhibits degradation of amino acid transporters, and positively regulates translation initiation by modulating the phosphorylation status of downstream effectors (16–19). Tor2p, in addition, regulates actin reorganization via activation of Rom2p, a GTP exchange factor for the small GTPases Rho1p and Rho2p (12, 13). Furthermore, Mss4p, a phosphatidylinositol 4-phosphate 5-kinase, and Plc1p, the yeast homolog of phospholipase C, have been implicated in the Tor signaling pathway suggesting a role for phosphoinositides and their metabolites in Tor function (21, 30). However, precisely how Tor1p and Tor2p are activated is not known, and no immediate downstream effectors that execute the Tor2p actin cytoskeleton function have been identified.

To gain a better understanding of Tor function, we examined the subcellular distribution of Tor1p and Tor2p and characterized domains within Tor2p that mediate localization. Here we show that Tor1p and Tor2p are peripheral membrane proteins that associate with the plasma membrane and a second compartment of high buoyant density. Tor localization to both

* This work was supported by grants from the Swiss National Science Foundation and the Canton of Basel (to M. N. H.). The costs of publication of this article were defrayed in part by the payment of page charges. This article must therefore be hereby marked "advertisement" in accordance with 18 U.S.C. Section 1734 solely to indicate this fact.

‡ Present address: Dept. of Pharmacology, University of Wisconsin Medical School, 1300 University Ave., Madison, WI 53706.

§ To whom correspondence should be addressed. Tel.: 41-61-267 21 50; Fax: 41-61-267 21 49; E-mail: M.Hall@unibas.ch.

¹ The abbreviations used are: Tor1, Tor2, target of rapamycin 1 and 2; HEAT, huntingtin, elongation factor 3, A subunit of phosphatase 2A, Tor1; FKBP12, FK506-binding protein; mTOR, mammalian target of rapamycin; 4E-BP1, eIF4E-binding protein 1; PAGE, polyacrylamide gel electrophoresis; HA, hemagglutinin; FITC, fluorescein isothiocyanate; kb, kilobase pairs; PIPES, 1,4-piperazinediethanesulfonic acid; DAPI, 4,6-diamidino-2-phenylindole; ER, endoplasmic reticulum; PM, plasma membrane; ConA, concanavalin A.

TABLE I
Yeast strains and plasmids

Strain	Genotype
JK9-3da	<i>MATa leu2-3,112 ura3-52 rme1 trp1 his4 GAL</i>
MH349-3d	<i>HMLa</i>
JK350-18a	<i>JK9-3da tor1::LEU2-4</i>
MB55-4b	<i>JK9-3da ade2 tor2::ADE2/pJK5</i> <i>MATa his4 tor2::ADE2 rot1-1</i>
Plasmid	Description
p6HIS-TOR1	=pAS12, <i>6HIS-TOR1</i> under control of the <i>GAL1</i> promoter in pSEY68 (<i>amp^rURA3 CEN</i>)
pHA-TOR1	=pYDF125, <i>HA-TOR1</i> under the control of the <i>GAL1</i> promoter (39)
p6HIS-TOR2	=pAS10, <i>6HIS-TOR2</i> under control of the <i>GAL1</i> promoter in pSEY68 (12)
pHA-TOR2	=pAS21, <i>HA-TOR2</i> under the control of the <i>GAL1</i> promoter in YCplac33 (<i>amp^rURA3 CEN</i>)
pTOR2(Δ 2463-2474)	=pJK13, <i>TOR2(Δ2463-2474)</i> under control of the <i>GAL1</i> promoter in pSEY68; made by replacing the corresponding wild-type fragment in <i>TOR2</i> with a 3.0-kb <i>SalI</i> restriction fragment of plasmid pJK10
pTOR2(Δ 1946-2474)	=pJK16, <i>TOR2(Δ1946-2474)</i> under control of the <i>GAL1</i> promoter in pSEY68; obtained by deletion of a 3.0-kb <i>SalI</i> restriction fragment from p6HIS-TOR2
pTOR2(Δ 1390-2474)	=pAS151, <i>TOR2(Δ1390-2474)</i> under control of the <i>GAL1</i> promoter in pSEY68; constructed by subcloning a 4.5-kb <i>SphI</i> restriction fragment obtained from plasmid pJK5 into the <i>SphI</i> site of plasmid pAS150
pTOR2(Δ 327-2474)	=pAS150, <i>TOR2(Δ327-2474)</i> under control of the <i>GAL1</i> promoter in pSEY68; a 1.0-kb fragment of <i>TOR2</i> was amplified by PCR using Vent polymerase and primers 5'-GATTCTGATCTTTACTTTC and 5'-CCTCTCGAGTGAAAAATGAATAAATACATTAAC. The resulting PCR product was cut with <i>XhoI</i> and <i>SphI</i> and subcloned into the <i>SalI</i> and <i>SphI</i> sites of pSEY68
pTOR2(Δ 327-1389)	=pAS152, <i>TOR2(Δ327-1389)</i> under control of the <i>GAL1</i> promoter in pSEY68; obtained by deleting the internal 4.5-kb <i>SphI</i> restriction fragment from plasmid p6HIS-TOR2
pTOR2(Δ 1-155)	=pJK19, <i>TOR2(Δ1-155)</i> under control of the <i>GAL1</i> promoter in pSEY68; obtained by PCR amplification of a 5.0-kb fragment of <i>TOR2</i> using Vent polymerase and primers 5'-CGGGATCCATGACTCTGATCTCATTCTACCTGAGTAC and 5'-GAGGAAGCGTTTGAGCTATCATA. The PCR product was cleaved with <i>BamHI</i> and subcloned into the <i>BamHI</i> site of pSEY68
pTOR2(Δ 1-326)	=pJK20, <i>TOR2(Δ1-326)</i> under control of the <i>GAL1</i> promoter in pSEY68; generated by PCR amplification of a 4.1-kb fragment of <i>TOR2</i> using Vent polymerase and primers 5'-CGGGATCCATG-GATTTCAGTGCATGCTACTC and 5'-GAGGAAGCGTTTGAGCTATCATA. The PCR product was cleaved with <i>BamHI</i> and subcloned into the <i>BamHI</i> site of pSEY68
pTOR2(Δ 1-1690)	=pJK43, <i>TOR2(Δ1-1690)</i> under control of the <i>GAL1</i> promoter in pSEY68; generated by deletion of a 4.8-kb <i>BamHI</i> restriction fragment from plasmid pJK5
pTOR2(487-2239)	=pJK41, <i>TOR2(487-2239)</i> under control of the <i>GAL1</i> promoter in pSEY68; generated by subcloning a 5.3-kb <i>BglII</i> restriction fragment into the <i>BamHI</i> site of pSEY68
pTOR2(326-1945)	=pJK27, <i>TOR2(326-1945)</i> under control of the <i>GAL1</i> promoter in pSEY68; generated by deleting a 3.0-kb <i>SalI</i> restriction fragment from plasmid pTOR2(Δ 1-326)
pJK5	<i>TOR2</i> under control of the <i>GAL1</i> promoter in pSEY68 (5)
pJK9	3.0-kb <i>SalI</i> fragment of <i>TOR2</i> in pSEY68 (<i>amp^rURA3 2μ</i>) (12)
pJK10	<i>BglII</i> deletion of plasmid pJK9
pJK14	Same as pJK9, but containing <i>TOR2Δ2463-2474</i> ; constructed by replacing the codon encoding C ₂₄₆₃ in <i>TOR2</i> with an AMBER codon by PCR overlap mutagenesis using mutagenic primers 5'-CCTATCCCAACATTATATCGGTTGGTCTCCATTC and 5'-GAATGGAGACCAACCGATATAATGTTGGGATAGG and flanking primers 5'-CCACAACGCATGATGCCA and 5'-GTCTTCACTTACGCCCTA spanning <i>BglII</i> sites in <i>TOR2</i> . The resulting PCR product was cleaved with <i>BglII</i> and subcloned into the <i>BglII</i> site of plasmid pJK10

compartments is likely via a soluble intermediate and, in the case of Tor2p, is independently mediated by multiple regions composed of HEAT repeats. HEAT repeat motifs have previously been implicated in mediating protein-protein interactions suggesting that Tor2p may be part of a membrane-associated protein complex.

EXPERIMENTAL PROCEDURES

Strains, Plasmids, Media, and Reagents—The complete genotypes of yeast strains and a description of the plasmids used in this study are listed in Table I. Yeast strains were grown at 30 °C unless otherwise indicated. The composition of rich (YP media) or synthetic minimal media (SD) supplemented with the appropriate nutrients was as described (31). Rapamycin (kindly provided by Sandoz Pharma, Basel) was kept as a stock solution (1 mg/ml in ethanol) at -80 °C and was added to the medium to a final concentration of 0.2 μ g/ml. Concanavalin A (fraction IV), aprotinin, chymostatin, leupeptin, pepstatin, and phenylmethylsulfonyl fluoride were obtained from Sigma. Recombinant lyticase was a gift from H. Riezman (Biozentrum, Basel). Zymolyase 20T was purchased from ICN Immunobiologicals (Irvine, CA). Protein A-Sepharose was from Amersham Pharmacia Biotech. Easytag EXPRE^{35S} protein labeling mix was purchased from PerkinElmer Life Sciences. Mouse monoclonal antibody HA.11 or rabbit polyclonal antibodies directed against the HA tag were purchased from Berkeley Antibody Co. (Berkeley, CA). FITC-conjugated goat anti-rabbit IgG, Texas Red-labeled streptavidin, and mouse monoclonal anti-Vph1 and

anti-alkaline phosphatase antisera were purchased from Molecular Probes (Eugene, OR). Rabbit anti-Cpy1p antiserum was kindly provided by S. Emr (University of California, San Diego); rabbit anti-Pma1p antiserum was from S. Gasser (Swiss Institute for Experimental Cancer Research, Lausanne, Switzerland); rabbit anti-Emp47p was provided by S. Schröder (Biozentrum, Basel, Switzerland); rabbit anti-Wbp1p antiserum was obtained from M. Aebi (ETH, Zürich, Switzerland); rabbit anti-hexokinase and anti-porin antisera were kindly provided by G. Schatz (Biozentrum, Basel, Switzerland).

Preparation of Polyclonal Antisera Directed against Tor1p and Tor2p—Polyclonal antisera against the C termini of Tor1p and Tor2p were raised against *Escherichia coli*-produced His₆-tagged fusion proteins containing amino acids 1680-2470 of Tor1p and amino acids 1683-2474 of Tor2p, respectively. To generate anti-peptide Tor2p antiserum, a synthetic peptide containing amino acids 16-29 of Tor2p (H₂N-Cys-Ser-Leu-Arg-Gln-Arg-Ala-Glu-Gly-Lys-His-Arg-Thr-Arg-Lys-COOH) was coupled to keyhole limpet hemocyanin by *N*-maleimidobenzoyl-*N*-hydrosuccinimide ester cross-linking. The resulting peptide/keyhole limpet hemocyanin conjugate or recombinant His₆-Tor1p and -Tor2p proteins were injected subcutaneously into female New Zealand White rabbits (SAVO, Germany). Injection of antigen in incomplete Freud's adjuvant was repeated at least five times, once every 4 weeks. The resulting antisera were tested and titered by Western blot and immunoprecipitation experiments of yeast cell extracts.

Cell Labeling and Biochemical Extraction of Tor—Unless otherwise indicated, yeast cells were grown at 30 °C in SD medium substituted with the appropriate amino acids and lacking methionine (SD-Met) to

an absorbance at 600 nm (A_{600}) of 0.5. Typically, 10 A_{600} units of cells were collected by centrifugation and resuspended in 1 ml of SD-Met medium. 120 μ Ci of Easytag EXPRE³⁵S³⁵S protein labeling mix were added, and cells were incubated for 20 min at 30 °C. A chase period was initiated by the addition of pre-warmed YPD medium (to A_{600} of 0.5), and incubation was continued for 30 min or as otherwise stated. The chase was terminated by addition of NaN_3 and NaF to a final concentration of 10 mM each. Cells were centrifuged and washed once in 10 mM NaN_3 , 10 mM NaF. Cell pellets were then resuspended in 15 ml of spheroplast I buffer (25 mM AMP-PIPES, pH 6.8, 0.6 M sorbitol, 140 mM cysteamine HCl, 5 mM EDTA, 10 mM NaN_3 , 10 mM NaF), incubated at room temperature for 10 min, collected by centrifugation, and converted to spheroplasts by lyticase digestion in spheroplast II buffer (25 mM AMP-PIPES, pH 6.8, 1.2 M sorbitol, 140 mM cysteamine HCl, 5 mM EDTA, 10 mM NaN_3 , 10 mM NaF) during a 60-min incubation at 30 °C. Spheroplasts were harvested by centrifugation at $500 \times g$ at 4 °C, resuspended in ice-cold lysis buffer (0.8 M sorbitol, 50 mM Tris-Cl, pH 7.5, 50 mM KOAc, 1 mM EDTA, 1 mM dithiothreitol, 1 μ g/ml aprotinin, 1 μ g/ml leupeptin, 1 μ g/ml pepstatin, 1 mM phenylmethylsulfonyl fluoride), and homogenized by pulling 10 times through a 23-gauge syringe. Unbroken cells were removed by centrifugation at $500 \times g$ at 4 °C for 10 min. To determine the nature of association of Tor proteins with the high speed 100,000 $\times g$ (P100) fraction, aliquots corresponding to 10 A_{600} of the cleared lysate were adjusted to 1 M NaCl, 1% Triton X-100, 1 M NaCl + 1% Triton X-100, 0.1 M NaCO_3 , pH 11.0, 5 M urea, 1 M hydroxylamine, pH 8.0, or left untreated. After incubation on ice for 10 min, the samples were subjected to a 100,000 $\times g$ spin for 45 min at 4 °C.

Immunoprecipitations, SDS-PAGE, and Western Blot Analysis—P13, P100, and PM fractions were directly resuspended in immunoprecipitation boiling buffer (50 mM Tris, pH 7.5, 1 mM EDTA, 1% SDS), whereas proteins present in the S100 supernatant fractions or in sucrose gradient fractions were first precipitated with trichloroacetic acid at a final concentration of 6%. Proteins were denatured by heating to 65 °C for 10 min and subjected to immunoprecipitation in 10 ml of TNET (1% Triton X-100, 100 mM Tris-Cl, pH 8.0, 100 mM NaCl, 5 mM EDTA). Fractions were first precleared by incubation with Sepharose CL-4B (Sigma), and then antiserum and protein A-Sepharose CL4B were added, and immunoprecipitations were incubated at 4 °C for 6 h to overnight with shaking. Tor1p and Tor2p were immunoprecipitated using the anti-Tor1p C-terminal antiserum and the anti-peptide Tor2p antiserum, respectively, except for the analysis of N-terminally truncated Tor2p mutants. In this case, the anti-Tor2p C-terminal antiserum was used. Antisera other than the anti-Tor1p or anti-Tor2p antisera were used according to personal recommendations to ensure quantitative immunoprecipitation of a given antigen. Immune complexes were recovered by centrifugation and washed five times with TNET before SDS-PAGE sample buffer was added. Samples were heated to 65 °C for 5 min to dissociate the immune complex. Immunoprecipitates were resolved by SDS-PAGE and analyzed and quantitated on a PhosphorImager using ImageQuant version 3.2 software (Molecular Dynamics, Sunnyvale, CA). Western blot analysis was performed using the ECL system and goat anti-mouse horseradish peroxidase-conjugated IgG as the secondary antibody (Amersham Pharmacia Biotech). Western blots were quantitated using densitometric scanning (Molecular Dynamics, Sunnyvale, CA).

Subcellular Fractionation and Sucrose Density Centrifugation—For differential fractionation and sucrose density centrifugation, cell-free extracts corresponding to 100 A_{600} of ³⁵S-labeled cells were prepared as described above and subjected to sequential centrifugations at 13,000 $\times g$ for 10 min at 4 °C and at 100,000 $\times g$ for 45 min at 4 °C. Aliquots of each fraction were removed for further analysis by immunoprecipitation. The remainder of the P13 and P100 pellet fractions was resuspended in 0.5 ml of 60% sucrose (w/w in 20 mM HEPES, pH 7.2), placed on the bottom of a Beckman ultraclear ultracentrifugation tube (Beckman Instruments, Fullerton, CA), and overlaid with 0.5-ml steps of 54, 50, 46, 42, 38, 34, 30, 26, 22, and 18% sucrose (w/w in 20 mM HEPES, pH 7.2). The gradients were centrifuged for 17 h at 170,000 $\times g$ in a TST55.1 rotor at 3 °C. After centrifugation, 0.33-ml fractions were collected manually from the top of the gradient. The pellet fraction was resuspended in the last fraction. The sucrose concentration was determined by measuring the refractive index.

For the analysis of Tor2p deletion variants, yeast cells carrying the mutant variants were grown overnight in selective raffinose medium, diluted into galactose medium (3% final concentration), and incubated an additional 4 h at 30 °C. 20 A_{600} units of cells were ³⁵S-labeled, chased, converted to spheroplasts, and lysed as described above. Cell-free extracts were prepared and separated into P13, P100, and S100

fractions as described above, and the distribution of Tor2 deletion variants was determined by immunoprecipitation and analysis on the PhosphorImager.

Preparation of Plasma Membrane Fractions and Pulse-Chase Experiments—Aliquots of 40 A_{600} units of yeast cells were labeled with Easytag EXPRE³⁵S³⁵S protein labeling mix for 1 min at 30 °C, collected by centrifugation for 2 s in a microcentrifuge, resuspended in 50 ml of pre-warmed YPD medium, and incubated at 30 °C. Cells were harvested after 15, 30, and 60 min after initiating the chase, resuspended in 10 mM NaN_3 , 10 mM NaF supplemented with cycloheximide (10 μ g/ml) to inhibit new protein synthesis, and kept on ice. Cells from the 0-min time point were directly resuspended in 10 mM NaN_3 , 10 mM NaF containing cycloheximide (10 μ g/ml) and kept on ice. Cells from each time point were then converted to spheroplasts, coated with ConA in the presence of cycloheximide, washed, and resuspended in ice-cold lysis buffer essentially as described (32). Extracts were homogenized by pulling 10 times through a 23-gauge needle. The low speed plasma membrane (PM) fraction, and the high speed P100 and S100 fractions were obtained by sequential centrifugation as described (32). The extent of cell lysis was determined by analyzing the percent of the cytosolic protein hexokinase that was recovered in the PM and P100 fractions. The amount of radioactivity in the PM, P100, and S100 fractions was expressed as percent of total radioactivity in the lysate after correction for cell lysis.

Indirect Immunofluorescence Microscopy—For visualization of HA-Tor1p and HA-Tor2p, yeast cells transformed with plasmid pYDF125 or pAS21 were grown overnight under selective conditions in S Raffinose medium, diluted into YPGal medium to induce expression of the HA fusion proteins, and cells were grown for 4–5 h to early logarithmic phase at 30 °C. This resulted in a 4–5-fold overexpression of the tagged protein compared with endogenous protein as estimated by Western blot analysis of cell extracts. Indirect immunofluorescence on whole fixed yeast cells was performed using standard procedures (18). HA-Tor1p and HA-Tor2p were visualized by anti-HA mouse monoclonal antibody HA.11 followed by FITC-conjugated goat anti-mouse IgG. For double labeling, HA-Tor1p and HA-Tor2p were visualized by anti-HA rabbit polyclonal antibodies followed by FITC-conjugated goat anti-rabbit IgG. Alkaline phosphatase was visualized by incubation with a monoclonal mouse anti-alkaline phosphatase antibody followed by biotinylated secondary antibody in combination with Texas Red-labeled streptavidin. DNA was stained with DAPI. The samples were viewed through a 60 \times lens using a Zeiss axioplan microscope (Carl Zeiss, Inc., Thornwood, NY). Confocal sections were collected using a laser-scanning confocal microscope consisting of a Bio-Rad MR 1000 scanhead mounted transversely to an inverted Nikon Diaphot 200. The microscope was controlled by the Bio-Rad's Lasesharp 3.0 program, which provided data acquisition and processing.

RESULTS

Detection of Tor1p and Tor2p—To aid in the molecular analysis of Tor function, we generated antibodies that specifically recognize Tor1p or Tor2p. Tor1p-specific antibodies were raised against the C-terminal kinase domain of Tor1p, whereas the antiserum against Tor2p was raised against a synthetic peptide corresponding to a unique N-terminal sequence of Tor2p. The anti-Tor1p antiserum immunoprecipitated a single polypeptide with an apparent molecular mass of 250 kDa (predicted size, 284 kDa) from ³⁵S-labeled wild-type extracts (Fig. 1A, lane 1). The same protein was also isolated from extracts derived from cells harboring a *tor2* disruption (Fig. 1A, lane 3) but not from extracts generated from cells that carried a *tor1* deletion mutation (Fig. 1A, lane 2). When *TOR1* was overexpressed under the control of the *GAL1* promoter, up to 5-fold higher levels of the 250-kDa species were recovered (data not shown), whereas no protein was immunoprecipitated with pre-immune serum (data not shown).

The anti-Tor2p antiserum specifically immunoprecipitated a single protein that migrated at approximately 250 kDa (predicted mass, 285 kDa) from ³⁵S-labeled wild-type cells (Fig. 1B, lane 1). This protein was also immunoprecipitated from an extract derived from a *tor1* disruption strain (Fig. 1B, lane 2) but not from an extract generated from a *tor2* mutant strain (Fig. 1B, lane 3). A 170-kDa polypeptide was immunoprecipitated from this strain instead, which corresponds in its mass to

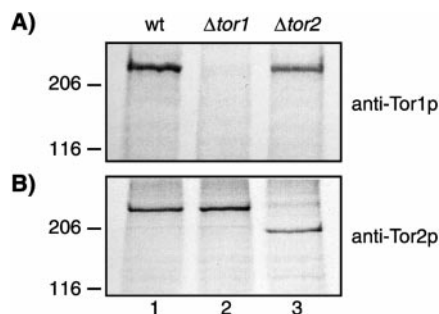


FIG. 1. Identification of Tor1p and Tor2p. Lysates prepared from 10 A_{600} of ^{35}S -labeled wild-type (*wt*; strain JK9-3da) cells or cells containing either a *tor1* (Δtor1 , strain MH349-3b) or a *tor2* (Δtor2 ; strain MB55-4b) deletion mutation were subjected to denaturing immunoprecipitation using polyclonal anti-Tor1p or anti-Tor2p antibodies. Immunoprecipitates were resolved by SDS-PAGE and analyzed on the PhosphorImager. The position and molecular weights ($\times 10^3$) of prestained standards are indicated at the left. MB55-4b also contains a mutation in the *ROT1* gene that allows *tor2*-deficient cells to live (53).

the predicted truncated Tor2p protein encompassing the N terminus up to the insertion point of the *ADE2* disruption marker (Fig. 1B, lane 3). Overexpression of *TOR2* on a multicopy plasmid led to the recovery of up to 10-fold stronger signal (data not shown). The 250-kDa species was, however, not recovered when preimmune serum was used or when excess peptide against which the anti-Tor2p antibodies were raised was present during immunoprecipitation (data not shown). Taken together, these results demonstrate that the anti-Tor1p and anti-Tor2p antisera specifically recognize endogenous Tor1p and Tor2p, respectively.

Tor1p and Tor2p Fractionate as Peripheral Membrane Proteins—As a first step to localize Tor1p and Tor2p, a ^{35}S -labeled extract derived from wild-type cells was fractionated into 100,000 $\times g$ cytosolic supernatant (S100) and membrane-enriched particulate (P100) fractions. These fractions were probed by immunoprecipitation for the presence of Tor1p and Tor2p. We found that Tor1p and Tor2p mainly partition into the particulate fraction (Fig. 2 and Table II) with only minor amounts (5–10% of either Tor1p or Tor2p) detected in the soluble fraction. Overexpression of Tor1p or Tor2p led to the recovery of higher levels of Tor proteins in the soluble fraction (20–30% in the Tor overproducing cells (Table II) compared with 5–10% in wild-type cells) which could indicate that association of Tor with the particulate fraction is saturable.

To determine the nature of the association of Tor protein with the particulate fraction, a ^{35}S -labeled extract was divided into aliquots and treated with a set of reagents prior to centrifugation at 100,000 $\times g$. The distribution of Tor1p, Tor2p, and the integral plasma membrane H^+ -ATPase Pma1p between the P100 and S100 fractions was then monitored by immunoprecipitation. As expected, Pma1p was extracted into the S100 fraction only by treatment with the nonionic detergent Triton X-100, but not by reagents that disrupt protein-protein interactions (Table II). In contrast, Tor1p and Tor2p were only partially extracted with Triton X-100 (1%) (Fig. 2 and Table II), whereas high salt (1 M NaCl), alkaline pH (0.1 M NaCO_3 , pH 11), or the chaotropic agent urea which disrupts protein-protein interactions released the majority of Tor1p and Tor2p into the soluble fraction (Fig. 2 and Table II). 1 M hydroxylamine, which cleaves thioester bonds between fatty acids and proteins (33), did not solubilize Tor1p or Tor2p (data not shown). These data together suggest that Tor1p and Tor2p are peripheral membrane proteins. This is consistent with the absence of predicted signal sequences or transmembrane domains in Tor1p and Tor2p.

Tor1p and Tor2p Localize to the Plasma Membrane and a

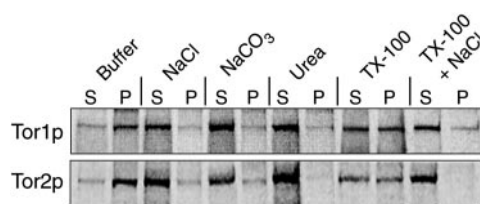


FIG. 2. Tor1p and Tor2p fractionate as peripheral membrane proteins. A cell extract prepared from 60 A_{600} of ^{35}S -labeled wild-type yeast cells was divided into aliquots and treated with the indicated reagent for 10 min on ice as described under “Experimental Procedures.” Extracts were then separated into 100,000 $\times g$ supernatant and pellet fractions, and Tor1p and Tor2p were immunoprecipitated from these fractions, resolved by SDS-PAGE, and analyzed on the PhosphorImager. S and P denote the 100,000 $\times g$ supernatant and pellet fractions, respectively. The position and molecular weights ($\times 10^3$) of prestained standards are indicated at the left. TX-100, Triton X-100.

Second Subcellular Compartment—Subcellular fractionation studies were carried out to identify more precisely the intracellular location of Tor1p and Tor2p. Wild-type cells were pulse-labeled with [^{35}S]Met/Cys, converted to spheroplasts, osmotically lysed, and unbroken cells were removed by low speed centrifugation. The cell-free extract was then sequentially centrifuged at 13,000 and 100,000 $\times g$ to generate the membrane-enriched particulate P13 and P100 fractions, as well as the cytosolic S100 supernatant fraction. The presence of Tor1p and Tor2p, as well as of a set of organelle marker proteins was determined in each fraction by immunoprecipitation.

The P13 fraction is highly enriched for plasma membrane, endoplasmic reticulum (ER), vacuoles, and mitochondria, whereas the P100 fraction is highly enriched for Golgi, endosomes, and secretory vesicles (Table III (34)). We found that almost all of the plasma membrane marker Pma1p, the ER membrane marker Wbp1p, the vacuolar membrane marker Vph1, and the mitochondrial outer membrane marker porin were present in the P13 fraction (Table III). The Golgi membrane marker Emp47p, in contrast, was almost exclusively found in the P100 fraction (Table III). The portion of Emp47p in the P13 fraction represents the ER-localized precursor form that is typically detected under the growth conditions used for these experiments (35). Tor1p or Tor2p were found to distribute equally between the P13 and P100 pellet fractions with only trace amounts present in the soluble fraction (Table III). The fractionation behavior of Tor1p and Tor2p is therefore different from that observed for specific organelle markers and could indicate that Tor proteins are present in more than one compartment.

To identify the subcellular membranous compartment(s) with which Tor1p and Tor2p associate, P13 and P100 fractions were resuspended in 60% sucrose and subfractionated by equilibrium flotation in continuous 18–54% sucrose density gradients. The gradients were fractionated and analyzed for the distribution of Tor1p, Tor2p, and various organelle markers. Tor1p and Tor2p present in the P13 fraction cofractionated with each other and the plasma membrane marker Pma1p (Fig. 3). Both Tor proteins clearly fractionated in a manner distinct from vacuolar (Cpy1p) and mitochondrial (porin) markers and were also partially resolved from the ER membrane marker Wbp1p (Fig. 3A and data not shown). In the P100 fraction, Tor1p and Tor2p were present in fractions that were clearly distinct from fractions containing the Golgi marker Emp47p (Fig. 3B). Furthermore, both Tor proteins were again at least partially resolved from the ER marker Wbp1p (Fig. 3B). Similar results were obtained when yeast extracts were resolved by velocity gradient centrifugation (data not shown). In summary, Tor1p and Tor2p appear to colocalize to two biochemically distinct subcellular compartments one of which

TABLE II
Association of Tor1p, Tor2p, and Pma1p with the particulate fraction

Wild-type cells were ³⁵S-labeled for 20 min, chased for 30 min at 30 °C and lysed, and the cell lysate was divided into equal aliquots and treated with the indicated reagents as described under "Experimental Procedures." After treatment, extracts were separated into S100 and P100 fractions, and the amounts of Tor proteins and Pma1p in each fraction were determined by quantitative immunoprecipitation and PhosphorImager analysis. Numbers indicate percent of total.

	Tor1p		Tor2p		Pma1p	
	S	P	S	P	S	P
		%		%		%
No treatment, endogenous	6	94	10	90	0	100
No treatment, <i>GALI</i> promoter	26	74	28	72		
High salt (1 M NaCl)	91	9	88	12	0	100
pH 11 (0.2 M NaCO ₃)	86	14	92	8	1	99
Urea (5 M)	97	3	93	7	1	99
Triton X-100 (1%)	46	54	49	51	70	30
Triton X-100 + high salt	98	2	95	5	81	19

S, supernatant; P, pellet.

TABLE III
Differential centrifugation

Wild-type cells were ³⁵S-labeled for 20 min, chased for 30 min at 30 °C, lysed, and subjected to differential centrifugation as described under "Experimental Procedures." The amount of Tor1p, Tor2p, and organelle markers in each fraction was determined by quantitative immunoprecipitation and PhosphorImager analysis. The amount of Vph1p was determined by Western blot analysis and densitometric scanning. Numbers indicate percent of total.

Marker protein	P13	P100	S100
	%	%	%
Tor1p	55	42	3
Tor2p	53	43	4
Pma1p (plasma membrane)	86	2	12
Wbp1p (endoplasmic reticulum)	78	20	2
Emp47p (Golgi)	8	90	2
Vph1p (vacuolar membrane)	95	3	2
Cpy1p (vacuolar lumen)	48	6	46
Porin (mitochondria)	97	2	1
Hexokinase (cytoplasm)	2	0	98

contains the plasma membrane.

We then purified plasma membrane by an independent method (32). This method is based on the coating of ³⁵S-labeled yeast spheroplasts with the lectin ConA that binds glycoproteins and selectively labels plasma membranes of intact cells. After cell lysis, the dense ConA-coated plasma membrane sheets can be separated from other cellular membranes by low speed centrifugation yielding the plasma membrane (PM) fraction. The low speed supernatant fraction is further separated into the particulate P100 and the cytosolic S100 fractions. By using this procedure, we were able to obtain a highly purified plasma membrane fraction (Fig. 4A) that contained only minor contamination by other organelle markers that was likely due to the presence of a small amount of unbroken cells in this fraction as evidenced by the cytosolic marker hexokinase. The majority of Tor1p and Tor2p copurified with plasma membrane. 50–65% of Tor1p and Tor2p was recovered in the PM fraction, whereas approximately 35–40% of Tor1p and Tor2p partitioned into the P100 fraction (Fig. 4A). Only trace amounts (5–10%) of Tor1p and Tor2p were detected in the cytosolic S100 fraction. We therefore conclude that more than half of Tor1p and Tor2p associates with the plasma membrane. The remaining portion of Tor is found in a different, high buoyant density fraction.

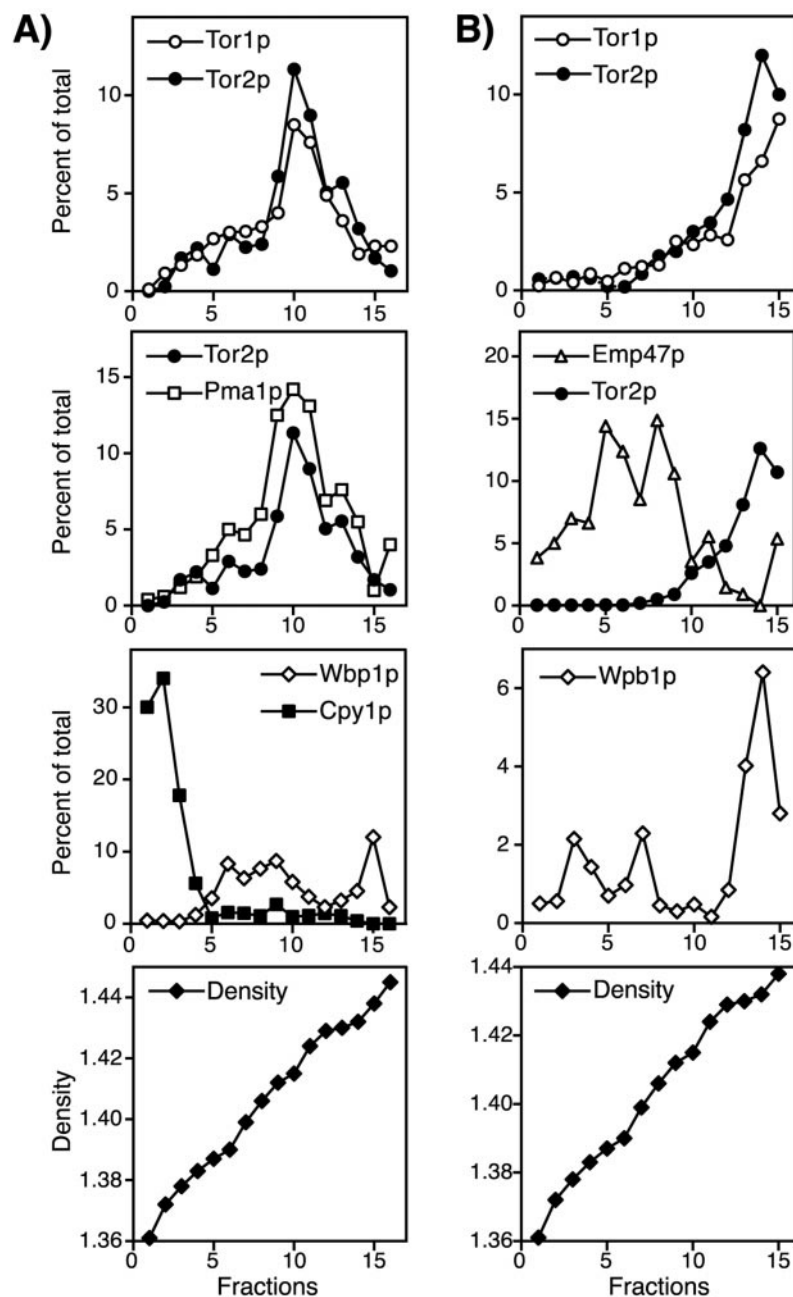
Tor1p and Tor2p Localization Is Rapid and Does Not Require Vesicle Transport—The presence of Tor1p and Tor2p in two distinct fractions may be explained by Tor passaging from one compartment to another. Alternatively, Tor1p and Tor2p could simultaneously associate with two compartments upon synthesis. To differentiate between these two possibilities, pulse-chase experiments were carried out with a labeling period of 1

min and increasing periods of chase with unlabeled amino acids. After the chase, cells were converted to spheroplasts and coated with ConA in the presence of cycloheximide to prevent new protein synthesis. Extracts were then generated and fractionated into PM, P100, and S100 fractions. We found that newly synthesized Tor1p and Tor2p rapidly partitioned into the PM and the P100 fractions (Fig. 4B). The majority of Tor1p and Tor2p was found in the PM and the P100 fractions even after only a 1-min pulse. The integral plasma membrane H⁺-ATPase Pma1p, in contrast, which is transported to the cell surface via the secretory pathway, starts to accumulate significantly in the PM fraction only after 15–30 min of chase (Fig. 4B).

We also analyzed the subcellular distribution of Tor1p and Tor2p in a set of mutants defective in various stages of the secretory (*sec4*), endocytic (*end4*), or Golgi to vacuole (*vps21*, *vps27*, *vps34*, and *vps45*) protein transport pathways (36–38). Cells were shifted to the nonpermissive temperature for 1 h to induce the mutant phenotype, pulse-labeled, lysed, and fractionated by differential centrifugation and velocity gradient centrifugation as described above. The intracellular distribution of Tor1p and Tor2p was analyzed and compared with that in wild-type cells. We found no changes in the fractionation profiles of Tor1p or Tor2p in these mutants (data not shown). Thus, together with our findings that functional vesicular transport pathways are not required for normal Tor localization, we conclude that Tor1p and Tor2p associate with both subcellular sites most likely via a soluble intermediate.

Rapamycin Does Not Affect the Subcellular Localization of Tor1p and Tor2p—We next investigated whether treatment of yeast cells with rapamycin alters the intracellular distribution of Tor1p or Tor2p. Wild-type cells were labeled with [³⁵S]Met/Cys for 20 min and chased with excess unlabeled amino acids in the presence of rapamycin (200 ng/ml) or carrier (ethanol) for 1 or 2 h at 30 °C. Microscopic examination of rapamycin-treated cells confirmed the effectiveness of rapamycin. After 1 h of rapamycin treatment, cells exhibited a marked increase in size and contained a single enlarged vacuole. After 2 h of treatment, cells were primarily arrested as large unbudded cells with large vacuoles (data not shown) as reported previously (4). Rapamycin-treated cells were converted to spheroplasts and coated with ConA to label the plasma membrane. ConA-coated plasma membrane (PM), particulate P100, and cytosolic S100 fractions were isolated and probed for the presence of Tor1p and Tor2p. Alternatively, extracts derived from rapamycin-treated cells were subjected to differential centrifugation and velocity gradient fractionation, and the fractionation profile of Tor1p and Tor2p was compared with that of cells treated with carrier alone. We found, by both methods, that rapamycin treatment did not affect Tor localization (Fig. 4B and data not

FIG. 3. Tor1p and Tor2p cofractionate with the plasma membrane marker Pma1p on sucrose density gradients. Wild-type cells were ^{35}S -labeled and fractionated into P13, P100, and S100 fractions as described under "Experimental Procedures." The P13 (A) and P100 (B) fractions were individually resuspended in 60% sucrose and resolved on a self-forming 18–54% sucrose density gradient. The sucrose gradients were fractionated manually from the top (fraction 1) to the bottom (fraction 15 or 16) in 0.33-ml fractions. The pellets were resuspended in the last fraction. Density was measured by refractometry. The distribution of Tor1p, Tor2p, and organelle marker proteins in each fraction was determined by quantitative immunoprecipitation and analysis on the PhosphorImager. Distribution of marker proteins is expressed as percent of the total pelletable counts (P13 + P100).



shown). Interestingly, rapamycin did appear to delay the transport of Pma1p to the cell surface indicating that the drug might affect the rate of secretion (Fig. 4B).

Localization of Epitope-tagged Tor1p and Tor2p by Immunofluorescence—We also used immunofluorescence as an independent method to localize Tors. Because our initial attempts to detect endogenous Tor proteins or GFP-Tor expressed under control of the endogenous promoter failed, Tor1p and Tor2p were tagged with the HA epitope at their N termini. The HA-Tor2p fusion protein complements the lethality of a *tor2* knock-out mutant² demonstrating that the tag does not interfere with Tor2p function. HA-Tor1p was previously shown to be functional *in vivo* (39). Furthermore, HA-Tor2p cofractionated with endogenous Tor2p during differential centrifugation and in sucrose density gradients, demonstrating that overexpression does not significantly alter subcellular localization (data

not shown). Thus, HA-Tor should accurately reflect the localization of the endogenous protein.

Visualization of HA-Tor1p and HA-Tor2p using monoclonal anti-HA antibodies revealed a discrete punctate staining at the cell periphery, as well as a less pronounced internal dot-like staining (Fig. 5A, and data not shown). No signal was detected in yeast cells overexpressing untagged Tor protein (data not shown). Comparison of the anti-HA and DAPI stainings showed that HA-Tor1p and HA-Tor2p do not localize to the nucleus or the perinuclear area (Fig. 5B, and data not shown). Furthermore, neither HA-Tor1p nor HA-Tor2p appears to colocalize with the vacuolar marker alkaline phosphatase (Fig. 5, D and E). Confocal microscopy demonstrated that the majority of HA-Tor1p and HA-Tor2p is localized to the plasma membrane, whereas the remaining portion is distributed throughout the cell interior in a dot-like pattern (Fig. 5, F and G). Thus, our immunofluorescence studies are in agreement with our biochemical fractionation studies and suggest that Tors are associated with the plasma membrane and another, as yet

² J. Kunz, U. Schneider, I. Howald, A. Schmidt, and M. N. Hall, unpublished results.

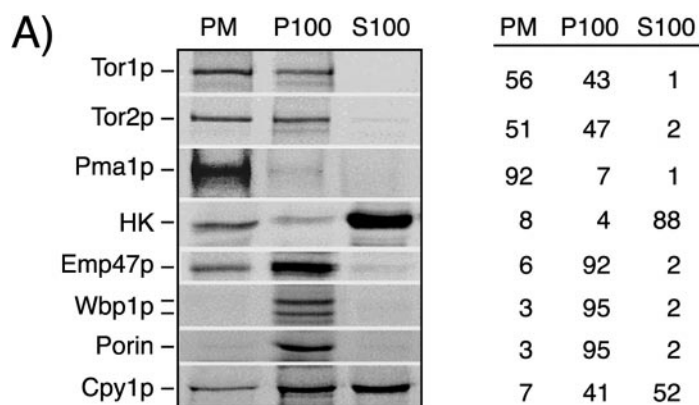
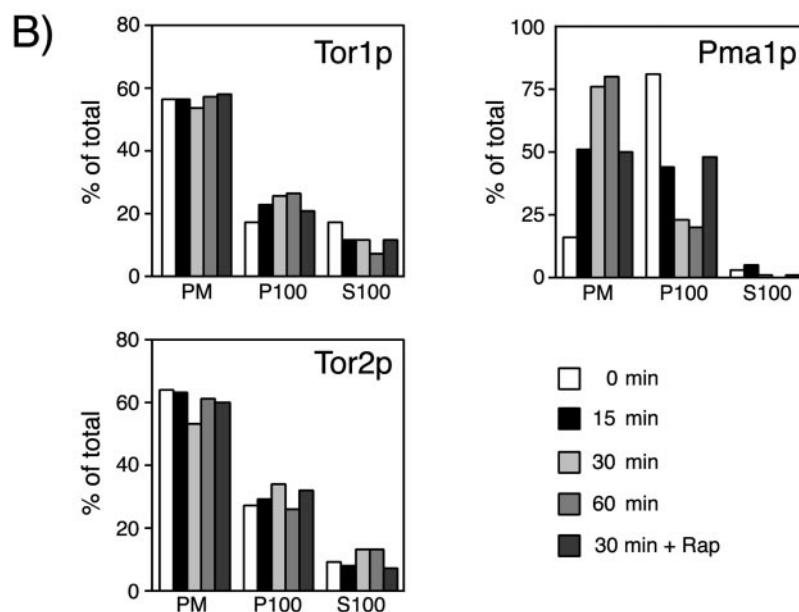


FIG. 4. Tor1p and Tor2p associate with plasma membrane via soluble intermediate. *A*, 20 A_{600} of wild-type cells were labeled with ^{35}S for 20 min, chased for 30 min, and PM, membrane-enriched P100, and cytosolic S100 fractions were prepared as described under "Experimental Procedures." Fractions were probed for Tor1p, Tor2p, and organelle markers by immunoprecipitation. Immunoprecipitates were resolved by SDS-PAGE and analyzed on the PhosphorImager. *B*, time course of Tor1p, Tor2p, or Pma1p association with the PM, the membrane-enriched P100, and the cytosolic S100 fractions. PM, P100, and S100 fractions from 40 A_{600} of pulse-labeled ConA-coated spheroplasts were prepared as described under "Experimental Procedures" and probed for Tor1p, Tor2p, and Pma1p by immunoprecipitation. Immunoprecipitates were resolved by SDS-PAGE and analyzed on the PhosphorImager.



unidentified, location.

Two Regions Containing HEAT Repeats Independently Mediate Tor2p Localization—To define the region(s) within Tor2p that mediates localization, we constructed deletion variants of Tor2p, and we tested their ability to associate with the particulate P13 and P100 fractions (summarized in Fig. 6). We found that an N-terminal fragment containing amino acids 1–326 (Tor2p Δ 327–2474) was sufficient for Tor2p localization. This fragment appeared to be unstable in yeast, yet associated with the P13 and P100 fractions in a manner similar to the wild-type protein. In accordance with this, an internal deletion mutant, which contained the N-terminal 326 amino acids but lacked a central domain (Tor2p Δ 327–1389), was stable and behaved identically in fractionation experiments. The C-terminal kinase homology domain, as well as the FKBP12-rapamycin binding domain, however, were not required for association of Tor2p with the P13 and P100 fractions (Tor2p Δ 1690–2474 and Tor2p Δ 1390–2474).

The N-terminal domain is sufficient but not necessary to mediate localization. Deletion of amino acids 1–326 did not result in mislocalization of Tor2p (Tor2p Δ 1–326). This indicates that a second domain within Tor2p independently mediates membrane association and localization. This second region is located between amino acids 327 and 1690, since a deletion mutant (Tor2p Δ 1–1690) lacking this region failed to fractionate with the P100 fraction and partitioned entirely into the P13

fraction. This could have indicated that this truncation mutant still associates with the plasma membrane but lacks the information for localization to the second compartment. However, when analyzed by equilibrium density gradient centrifugation, Tor2p Δ 1–1690 failed to cofractionate with wild-type Tor2p but rather segregated into a denser part of the gradient (data not shown). This suggests that the information for proper subcellular localization is lost in this mutant and that the protein aberrantly associates with another subcellular compartment. Further analysis of Tor2p deletion variants (Tor2p Δ 1390–2474, Tor2p Δ 487–2239, and Tor2p Δ 326–1945) restricted the second domain contributing to Tor2p localization to a region between amino acids 487 and 1690. In summary, these data indicate that localization of Tor2p involves two regions that do not include the kinase domain or the FKBP12-rapamycin-binding site but contain extensive repeats, termed HEAT repeats (see below). These HEAT repeat domains can independently mediate association of Tor2p with both intracellular sites.

DISCUSSION

We investigated the subcellular distribution of Tor1p and Tor2p by biochemical and immunofluorescence approaches, and we found that Tor1p and Tor2p similarly distribute to two biochemically distinct fractions. We have identified one of these fractions as the plasma membrane. The majority of Tor1p and Tor2p cofractionated with the integral plasma membrane

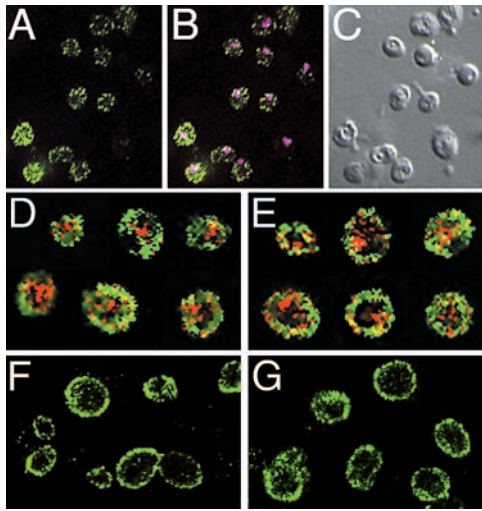


FIG. 5. Intracellular localization of Tor1p and Tor2p. Wild-type yeast cells transformed with vectors containing *HA-TOR1* or *HA-TOR2* under the control of the inducible *GAL1* promoter were grown at 30 °C in medium containing glycerol as the carbon source and then shifted to medium containing galactose to induce expression of the fusion protein. Cells were incubated for 4–5 h at 30 °C before being fixed and processed for immunofluorescence. *A*, indirect immunofluorescence showing HA-Tor2p; *B*, HA-Tor2p (green) overlaid with DAPI staining (purple) to visualize nuclei; *C*, Nomarski optics to visualize cells; *D*, HA-Tor1p (green) overlaid with alkaline phosphatase staining (red) to visualize vacuoles; *E*, HA-Tor2p (green) overlaid with alkaline phosphatase staining (red); *F*, confocal slice of cells expressing HA-Tor1p; *G*, confocal slice of cells expressing HA-Tor2p.

marker Pma1p during differential centrifugation studies and on sucrose density equilibrium gradients. Association with plasma membrane was further substantiated by an independent procedure using the lectin ConA that selectively binds to glycoproteins on intact yeast spheroplasts and allows the purification of highly enriched plasma membrane sheets. 50–65% of Tor1p and Tor2p was found to purify with plasma membrane, whereas other organelle markers could be clearly separated from this fraction. In agreement with the biochemical data, immunofluorescence staining of HA-Tor1p and HA-Tor2p was detected at discrete sites at the cell periphery and in a punctate pattern throughout the cytoplasm.

The localization of Tor1p and Tor2p to the plasma membrane is consistent with their function. One function of Tor2p is to control organization of the actin cytoskeleton by activation of a GTPase switch composed of Rho1p, Rho2p, and the GDP/GTP exchange factor Rom2p (12, 13). A second function of Tor2p that is shared with Tor1p is to regulate translation initiation and G₁ progression in response to nutrient availability in yeast. Both Rom2p and Rho1p have been localized to the plasma membrane, and Rho1p in addition has also been detected on Golgi structures and post-Golgi vesicles (40–42). Furthermore, Mss4p, an essential phosphatidylinositol 4-phosphate 5-kinase and candidate component of the Tor signaling pathway, is also localized to the plasma membrane (21, 43, 44). In addition, Plc1p, the yeast homolog of phospholipase C, has been linked to both Tor2p functions and may mediate generation of lipid second messengers at the plasma membrane (21, 30). The localization of Tor proteins to the plasma membrane is therefore consistent with the localization of known or suspected downstream effectors.

How localization of Tor1p and Tor2p to a second subcellular site may relate to their function as well as the nature of this site remains to be determined. Our subcellular fractionation and indirect immunofluorescence studies demonstrate that this second site is distinct from mitochondria, nuclei, Golgi, and

vacuoles. Further studies will be required to determine whether Tor proteins associate with membranes of high buoyant density or with a large protein complex, both of which could be expected to partition into the P100 fraction.

Cardenas *et al.* (45) have reported previously that Tor2p is localized to the surface of yeast vacuoles and that this association is disrupted by the immunosuppressive drug rapamycin. This is in contrast to our results, which show that Tor proteins are localized to the plasma membrane and a second compartment, which is biochemically distinct from the vacuole. Furthermore, we do not observe an effect of rapamycin on Tor localization. The reason for the discrepancy between their results and ours is not known at present. However, we base our interpretation on several observations. (a) We have demonstrated that our antisera specifically recognize endogenous Tor1p or Tor2p and do not cross-react. (b) Our biochemical fractionation data are consistent with findings obtained by direct purification of plasma membrane and results obtained by immunofluorescence studies using epitope-tagged Tor1p and Tor2p. (c) We do not observe any immediate effects of rapamycin on Tor2p localization as judged by several independent methods including differential centrifugation,² sucrose density gradient centrifugation,² purification of plasma membrane, and indirect immunofluorescence.

How do Tor proteins become membrane-bound and reach their subcellular location? Our extraction data suggest that at least part of Tor1p and Tor2p are peripheral membrane proteins. Only reagents that disrupt protein-protein interactions efficiently extract the Tor proteins into a soluble fraction. The reproducible effect of detergent extraction suggests that the association of Tor1p and Tor2p with membranes may be complex and may involve both ionic and hydrophobic protein-protein interactions with a membrane-bound protein(s) or even protein-lipid interactions. Pulse-chase experiments indicate that Tor1p and Tor2p associate rapidly and simultaneously with their final destinations and that this association is most likely via a soluble intermediate. This is in accordance with our finding that Tor localization is not altered in yeast mutants that are defective for endocytic, secretory, or Golgi to vacuole vesicle trafficking pathways. Thus, association of Tor proteins with membranes is likely mediated by interaction with an integral membrane protein or with a membrane-associated protein complex.

We used deletion analysis of *TOR2* to identify the region(s) that mediate localization and, potentially, may engage in protein-protein interaction. This analysis identified two domains, in the N terminus and center of Tor2p, that independently mediate localization. The most prominent feature in these domains is an extensive stretch of sequence composed of a repeated antiparallel α -helical motif, termed HEAT repeat motif (46). These repeats extend in two blocks (amino acids 100–470 and 560–1220) and encompass the two regions identified by our deletion analysis as sufficient for mediating localization. Because Tor1p colocalizes with Tor2p and also contains HEAT repeats (1, 46), it is likely that similar findings apply to its localization.

HEAT repeat motifs are highly divergent and have been detected in a number of proteins, including huntingtin, elongation factor 3, the 65-kDa structural A subunit of protein phosphatase 2A (PP2A R65/A), the nuclear pore transport protein importin β , and the splicing factor SAP155, for example, many of which have a demonstrated or suspected role in vesicular or protein traffic and form multiprotein complexes (46, 47). The three-dimensional structure of the HEAT repeats in several of these proteins has been recently solved and reveals an extended curved conformation composed of a double layer of

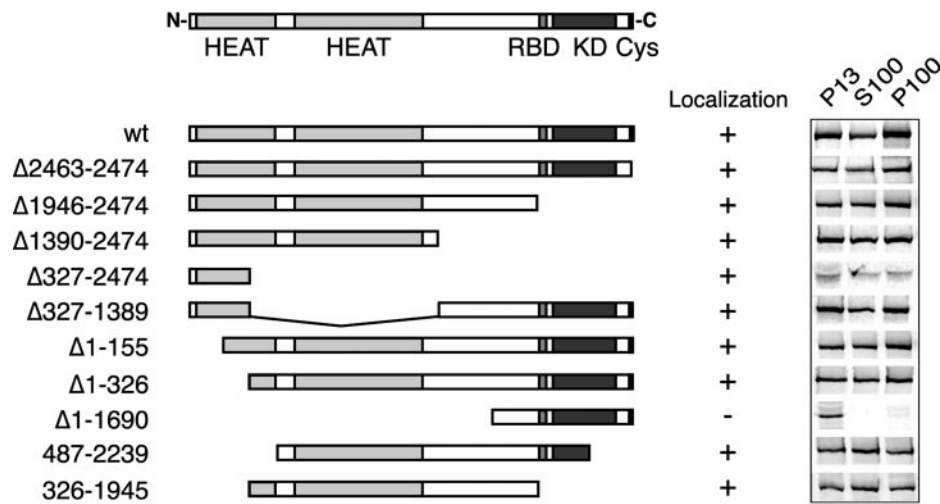


FIG. 6. Identification of Tor2p domains that mediate association with the particulate fractions. A schematic representation showing Tor2p and the boundaries of Tor2p deletion mutants. The structure of Tor2p is presented on top. Regions indicated are the HEAT repeat-containing domains (HEAT), the FKBP12-rapamycin-binding domain (RBD), the kinase homology domain (KD), and the cysteine-rich motif at the C terminus (CYS). The region present in each deletion mutant is depicted below. Amino acid residues present or lacking (Δ) in these mutants are indicated on the left. Tor2p or deletion variants thereof expressed under the control of the *GALI* promoter were tested for their ability to associate with the particulate P13 and P100 fractions. 35 S-labeled cell extracts were fractionated by differential centrifugation into P13, P100, and S100 fractions, and Tor2p or Tor2p deletion variants present in these fractions were immunoprecipitated, resolved by SDS-PAGE, and analyzed on the PhosphorImager. Plus and minus signs indicate the ability or inability, respectively, of each mutant to associate with P13 and P100 fractions in a manner quantitatively similar to the wild-type protein.

α -helices (48–51). This structure provides a large exposed surface with a hydrophobic nature that can participate in multiple protein-protein interactions. Structural data in combination with biochemical and deletion analysis indicate that groups of HEAT repeats indeed mediate interactions with distinct binding partners (48–51).

HEAT repeats domains may, therefore, anchor Tor to the membrane by mediating interactions with membrane-associated protein(s). The large and extended surface formed by these repeats may also provide additional protein-protein interaction interfaces with effectors or regulatory components. In accordance with such a hypothesis, we found that overexpression of the central region containing HEAT repeats is detrimental to yeast cells by interfering with Tor2p function.²

Striking parallels also exist between Tor2p and other proteins containing HEAT repeats. Huntingtin, the protein affected in Huntington's disease, is a large protein that is localized to multiple subcellular compartments, including vesicular structures, and interacts with a plethora of proteins involved in actin cytoskeleton function and possibly vesicular transport (47). Furthermore, ATM, a Tor-related protein, is localized to the nucleus and cytoplasmic vesicles and was recently shown to bind β -adaptin, a protein involved in clathrin-mediated endocytosis (52).

It is therefore tempting to speculate that HEAT repeats in Tor proteins act as molecular scaffolds for the recruitment of signaling complexes. The large interaction surface in these proteins and their localization to multiple cellular compartments may provide a means to integrate several inputs and to relay signals regulating temporal as well as spatial growth. An important issue now becomes identification of Tor-interacting protein(s). Definition of minimal domains that mediate localization should facilitate the isolation of protein(s) that anchor Tor to membranes and may potentially lead to the identification of regulators and additional effectors of the Tor pathway.

Acknowledgments—We thank Stephan Schröder for advice and reagents; Thomas Aust for the gift of lyticase; Scott Emr, Susan Gasser, Markus Aebi, Gottfried Schatz, Gerald Crabtree, and Tom Stevens for the generous gift of plasmids and antibodies; Howard Riezman for yeast

strains, reagents, and discussions; and Georg Halder for comments on the manuscript.

REFERENCES

- Dennis, P. B., Fumagalli, S., and Thomas, G. (1999) *Curr. Opin. Genet. & Dev.* **9**, 49–54
- Thomas, G., and Hall, M. N. (1997) *Curr. Opin. Cell Biol.* **9**, 782–787
- Cafferkey, R., Young, T. R., McLaughlin, M. M., Bergsma, D. J., Koltin, Y., Sathe, G. M., Faucette, L., Eng, W. K., Johnson, R. K., and Livi, G. P. (1993) *Mol. Cell. Biol.* **13**, 6012–6023
- Heitman, J., Movva, N. R., and Hall, M. N. (1991) *Science* **253**, 905–909
- Kunz, J., Henriquez, R., Schneider, U., Deuter-Reinhard, M., Movva, N. R., and Hall, M. N. (1993) *Cell* **73**, 585–596
- Stan, R., McLaughlin, M. M., Cafferkey, R., Johnson, R. K., Rosenberg, M., and Livi, G. P. (1994) *J. Biol. Chem.* **269**, 32027–32030
- Chen, J., Zheng, X. F., Brown, E. J., and Schreiber, S. L. (1995) *Proc. Natl. Acad. Sci. U. S. A.* **92**, 4947–4951
- Chiu, I. M., Katz, H., and Berlin, V. (1994) *Proc. Natl. Acad. Sci. U. S. A.* **91**, 12574–12578
- Sabatini, D. M., Erdjument-Bromage, H., Lui, M., Tempst, P., and Snyder, S. H. (1994) *Cell* **78**, 35–43
- Keith, C. T., and Schreiber, S. L. (1995) *Science* **270**, 50–51
- Hunter, T. (1995) *Cell* **83**, 1–4
- Schmidt, A., Kunz, J., and Hall, M. N. (1996) *Proc. Natl. Acad. Sci. U. S. A.* **93**, 13780–13785
- Schmidt, A., Bickle, M., Beck, T., and Hall, M. N. (1997) *Cell* **88**, 531–542
- Noda, T., and Oshumi, Y. (1998) *J. Biol. Chem.* **273**, 3963–3966
- Barbet, N. C., Schneider, U., Helliwell, S. B., Stanfield, I., Tuite, M. F., and Hall, M. N. (1996) *Mol. Biol. Cell* **7**, 25–42
- Schmidt, A., Beck, T., Koller, A., Kunz, J., and Hall, M. N. (1998) *EMBO J.* **17**, 6924–6931
- Hardwick, J. S., Kuruvilla, F. G., Tong, J. K., Shamji, A. F., and Schreiber, S. L. (1999) *Proc. Natl. Acad. Sci. U. S. A.* **96**, 14866–14870
- Beck, T., and Hall, M. N. (1999) *Nature* **402**, 689–692
- Cardenas, M. E., Cutler, N. S., Lorenz, M. C., Di Como, C. J., and Heitman, J. (1999) *Genes Dev.* **13**, 3271–3279
- Powers, T., and Walter, P. (1999) *Mol. Biol. Cell* **10**, 987–1000
- Helliwell, S. B., Howald, I., Barbet, N., and Hall, M. N. (1998) *Genetics* **148**, 99–112
- Brown, E. J., and Schreiber, S. L. (1996) *Cell* **86**, 517–520
- Hara, K., Yonezawa, K., Weng, Q. P., Kozlowski, M. T., Belham, C., and Avruch, J. (1998) *J. Biol. Chem.* **273**, 14484–14494
- Iiboshi, Y., Pabst, P. J., Kawasome, H., Hosoi, H., Abraham, R. T., Houghton, P. J., and Terada, N. (1999) *J. Biol. Chem.* **274**, 1092–1099
- Shigemitsu, K., Tsujishita, Y., Hara, K., Nanahoshi, M., Avruch, J., and Yonezawa, K. (1999) *J. Biol. Chem.* **274**, 1058–1065
- Brown, E. J., Beal, P. A., Keith, C. T., Chen, J., Shin, T. B., and Schreiber, S. L. (1995) *Nature* **377**, 441–446
- Di Como, C. J., and Arndt, K. T. (1996) *Genes Dev.* **10**, 1904–1916
- Murata, K., Wu, J., and Brautigan, D. L. (1997) *Proc. Natl. Acad. Sci. U. S. A.* **94**, 10624–10629
- Jiang, Y., and Broach, J. R. (1999) *EMBO J.* **18**, 2782–2792
- Alarcon, C. M., Heitman, J., and Cardenas, M. E. (1999) *Mol. Biol. Cell* **10**, 2531–2546

31. Sherman, F. (1991) in *Guide to Yeast Genetics and Molecular Biology* (Guthrie, C., and Fink, G. R., eds) pp. 3–20, Academic Press, Inc., San Diego, CA
32. Patton, J. L., and Lester, R. L. (1991) *J. Bacteriol.* **173**, 3101–3108
33. Magee, A. I., and Courtneidge, S. A. (1985) *EMBO J.* **4**, 1137–1144
34. Marcusson, E. G., Horazdovsky, B. F., Cereghino, J. L., Gharakhanian, E., and Emr, S. D. (1994) *Cell* **77**, 579–586
35. Schröder, S., Schimmöller, F., Singer-Krüger, B., and Riezman, H. (1995) *J. Cell Biol.* **131**, 895–912
36. Goud, B., Salminen, A., Walworth, N. C., and Novick, P. J. (1988) *Cell* **53**, 753–768
37. Raths, S., Rohrer, J., Crausaz, F., and Riezman, H. (1993) *J. Cell Biol.* **120**, 55–65
38. Schu, P. V., Takegawa, K., Fry, M. J., Stack, J. H., Waterfield, M. D., and Emr, S. D. (1993) *Science* **260**, 88–91
39. Fiorentino, D. F., and Crabtree, G. R. (1997) *Mol. Biol. Cell* **8**, 2519–2537
40. Manning, B. D., Padmanabha, R., and Snyder, M. (1997) *Mol. Biol. Cell* **8**, 1829–1844
41. Yamochi, W., Tanaka, K., Nonaka, H., Maeda, A., Musha, T., and Takai, Y. (1994) *J. Cell Biol.* **125**, 1077–1093
42. McCaffrey, M., Johnson, J. S., Goud, B., Myers, A. M., Rossier, J., Popoff, M. R., Madaule, P., and Boquet, P. (1991) *J. Cell Biol.* **115**, 309–319
43. Desrivieres, S., Cooke, F. T., Parker, P. J., and Hall, M. N. (1998) *J. Biol. Chem.* **273**, 15787–15793
44. Homma, K., Terui, S., Minemura, M., Qadota, H., Anraku, Y., Kanaho, Y., and Ohya, Y. (1998) *J. Biol. Chem.* **273**, 15779–15786
45. Cardenas, M. E., and Heitman, J. (1995) *EMBO J.* **14**, 5892–5907
46. Andrade, M. A., and Pork, P. (1995) *Nat. Genet.* **11**, 115–116
47. Gusella, J. F., and MacDonald, M. E. (1998) *Curr. Opin. Neurobiol.* **8**, 425–430
48. Groves, R. M., Hanlon, N., Turowski, P., Hemmings, B. A., and Barford, D. (1999) *Cell* **96**, 99–110
49. Cingolani, G., Petosa, C., Weis, K., and Müller, C. W. (1999) *Nature* **399**, 221–229
50. Chook, Y. M., and Blobel, G. (1999) *Nature* **399**, 230–237
51. Vetter, I. R., Arndt, A., Kutay, U., Görlich, D., and Wittinghofer, A. (1999) *Cell* **97**, 635–646
52. Lim, D.-S., Kirsch, D. G., Canman, C. E., Ahn, J.-H., Ziv, Y., Newman, L. S., Darnell, R. B., Shiloh, Y., and Kastan, M. B. (1998) *Proc. Natl. Acad. Sci. U. S. A.* **95**, 10146–10151
53. Bickle, M., Delley, P.-A., Schmidt, A., and Hall, M. N. (1998) *EMBO J.* **17**, 2235–2245

HEAT Repeats Mediate Plasma Membrane Localization of Tor2p in Yeast
Jeannette Kunz, Ulrich Schneider, Isabelle Howald, Anja Schmidt and Michael N. Hall

J. Biol. Chem. 2000, 275:37011-37020.

doi: 10.1074/jbc.M007296200 originally published online September 5, 2000

Access the most updated version of this article at doi: [10.1074/jbc.M007296200](https://doi.org/10.1074/jbc.M007296200)

Alerts:

- [When this article is cited](#)
- [When a correction for this article is posted](#)

[Click here](#) to choose from all of JBC's e-mail alerts

This article cites 52 references, 33 of which can be accessed free at <http://www.jbc.org/content/275/47/37011.full.html#ref-list-1>